ORGANIC CHEMISTRY FRONTIERS

RESEARCH ARTICLE

View Article Online
View Journal | View Issue

Cite this: *Org. Chem. Front.*, 2026, **13**, 96

Photoswitchable anion recognition *via* synergy between chalcogen bonding and hydrogen bonding

Qinhua Rao,[a,b] Hebo Ye,*[a] Peng He[a] and Lei You *[a,b,c]

Exploring photoresponsive noncovalent interactions with controllable tunability is of great significance for advancing supramolecular recognition and smart dynamic materials. Herein, we report light-responsive hydrazone-based receptors incorporating a telluroazole-derived chalcogen bond donor for photoswitchable anion binding. This system undergoes bidirectional *E*/*Z* photoisomerization, which modulates an intramolecular NH···N hydrogen bond and hence enhances the electrophilicity of the tellurium center in the *Z*-isomer for chalcogen bonding. This structural change leads to a significant increase in the binding affinity of the *Z*-isomer toward halide anions (Cl^-, Br^-, and I^-), with binding constants up to 20 times higher than the *E*-isomer. The incorporation of electron-withdrawing substituents amplifies the polarization, allowing the control over binding strength and selectivity. Moreover, anion binding facilitates $Z \rightarrow E$ photoisomerization, offering a feedback mechanism between recognition and structural switching. This study demonstrates a new strategy combining reversible photochemical control and synergistic noncovalent interaction modulation, offering an effective approach for the development of stimuli-responsive supramolecular systems.

Received 22nd September 2025,
Accepted 6th October 2025

DOI: 10.1039/d5qo01341k

rsc.li/frontiers-organic

Introduction

Stimuli-responsive molecular systems capable of reversibly modulating noncovalent interactions are essential for the construction of intelligent functional assemblies and materials.[1–11] Among various external stimuli, light has been attracting intensive attention in view of its non-invasive nature and high spatiotemporal resolution, enabling dynamic and active control over molecular conformations and recognition pockets.[12–17] Embedding photoresponsive units, such as photochromic switches, into receptor frameworks allows for reversible regulation of intramolecular/intermolecular forces, such as hydrogen bonding and host–guest recognition,[18–21] which has been widely applied in the development of supramolecular switches and molecular machines.[22–25] However, achieving efficient light-driven anion recognition remains challenging, primarily due to solvation effects, geometric mismatch, and inherently weak binding forces.[26–34] Recently, chalcogen bonding (ChB),[35–45] a blossoming type of noncovalent interaction with strong directionality and tunable electronic characteristics, has emerged as a promising alternative to hydrogen bonding (HB)[46–49] and halogen bonding (XB)[50–53] for anion recognition and associated endeavors, offering distinct selectivity and hydrophobicity. As a result, the development of novel structures and mechanisms for photoswitchable anion binding is highly desired.

To achieve photoresponsive anion recognition, various strategies have been developed that combine molecular photoswitches with anion binding motifs (Fig. 1). One established approach takes advantage of light-triggered *E*/*Z* switching of hydrazones and masking/unmasking of intramolecular HB (Fig. 1a).[54–57] Chmielewski reported an acylhydrazone-based heteroditopic ion pair receptor, wherein light-induced *E*/*Z* isomerization of the C=N bond controls the ON/OFF states of both cation and anion binding.[58] Very recently, an anion pump for active transport of chloride was established with a trimeric hydrazone photoswitch-based receptor by Aprahamian.[59] The so-called molecular tweezers offered diverse avenues for dynamically regulating binding affinity and selectivity by altering molecular conformation and spatial positioning of functional groups (Fig. 1b).[60] Integrating *E*/*Z* photoisomerizable units, such as azobenzene and stiff-stilbene, with HB/XB/ChB donors enables light-controlled anion recognition systems, as showcased by Feringa, Wezenberg, Langton, and others (Fig. 1b).[61–70] Zhang designed a visible-light-switchable

[a]*State Key Laboratory of Structural Chemistry, Fujian Institute of Research on the Structure of Matter, Chinese Academy of Sciences, Fuzhou 350002, China. E-mail: lyou@fjirsm.ac.cn, yehebo@fjirsm.ac.cn*
[b]*University of Chinese Academy of Sciences, Beijing 100049, China*
[c]*Fujian Science & Technology Innovation Laboratory for Optoelectronic Information of China, Fuzhou 350108, China*

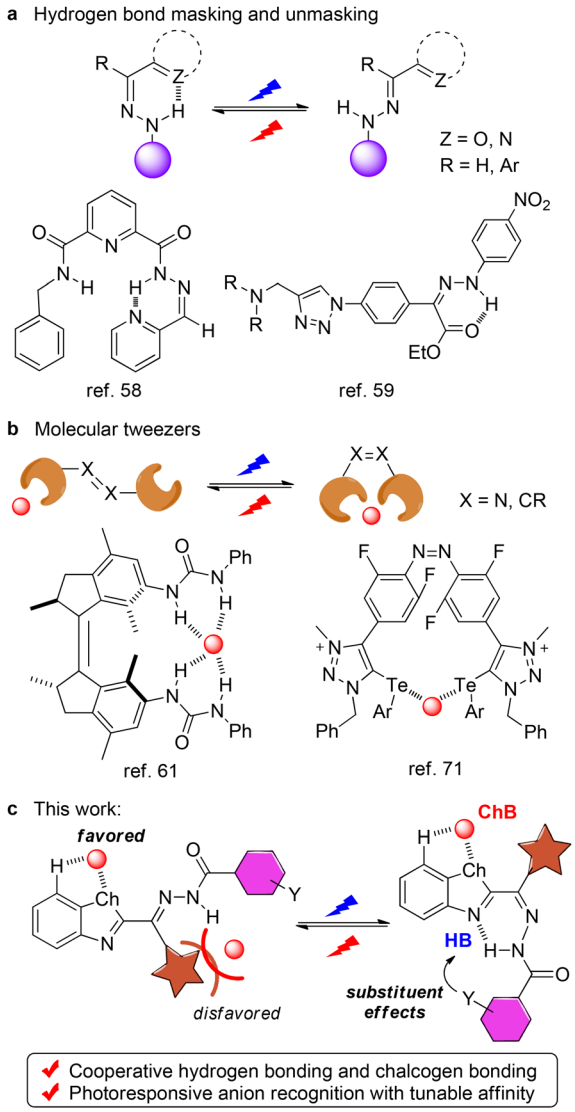

Fig. 1 Representative strategies for photoswitchable anion recognition. (a) HB masking/unmasking. (b) Molecular tweezers. (c) This work of ChB activated by intramolecular NH···N HB with telluroazole-derived hydrazones.

tellurium-based ChB system bearing azobenzene-linked tellurotriazole units for light-controlled halide binding and catalysis.[71] Through the incorporation of azobenzene into urea-derived anion coordination cages, photoresponsive anion binding and further tuning of *E*/*Z* isomerization properties were achieved by Wu and coworkers.[72] Despite elegant advances, the manipulation of cooperative effects between different types of noncovalent interactions for light-mediated anion receptors is virtually untouched.

With hydrazones as extensively studied molecular recognition motifs, dynamic covalent bonds, and configurational switches,[73–86] we postulated the introduction of the tellurazole group[87–89] into acylhydrazones toward the goal of constructing photoresponsive anion receptors (Fig. 1c). As the nearby nitrogen and tellurium sites can engage in HB and ChB, respectively, their potential synergy would impact anion binding. The changes in geometry and HB/ChB upon *E*/*Z* photoisomerization would therefore provide a potent platform for light-controlled anion recognition. In the current work, we report the development of a photoresponsive anion receptor system that integrates hydrazone photoswitches with a benzotellurazole-based chalcogen bond donor (Fig. 1c). Light-triggered $E \rightarrow Z$ isomerization induces the formation of the key intramolecular NH···N HB, which in turn enhances the electrophilicity of the chalcogen donor and strengthens its binding affinity toward halide anions. Furthermore, the use of electron-withdrawing substituents enables fine-tuning of binding strength and selectivity. Notably, the reverse $Z \rightarrow E$ isomerization is promoted by halide binding, revealing a feedback mechanism between anion recognition and *E*/*Z* switching. The strategy combines photochemical control and cooperative noncovalent interactions, offering versatile tools for light-regulated anion receptors.

Results and discussion

Synthesis and structures

To realize the design concept, a series of chalcogen-containing acylhydrazones was constructed *via* modular synthesis (Scheme S1 and Fig. S1–S27). The reaction of 2,2′-ditellanediyldianiline with phenylacetyl chloride yielded a benzyl-substituted benzotellurazole derivative. After oxidation to the corresponding ketone, condensation with the hydrazide afforded the desired photoswitch molecule (**1**) (Fig. 2a). The thiazole (**2**) and selenazole (**3**) derivatives were synthesized as controls, along with varied substituents in tellurium-containing hydrazones (**4–6**). The phenyl group was attached to the C=N as a "wall" to bias anion binding toward the chalcogen site (Fig. 1c). As a comparison, benzotellurazole-2-carboaldehyde derived acylhydrazone (**7**) was also prepared. The tellurole ester intermediate was synthesized by reacting 2,2′-ditellanediyldianiline with diethyl oxalate. Subsequently, sodium borohydride reduction to give the alcohol and then oxidation with 2-iodoxybenzoic acid (IBX) afforded the aldehyde, which was then condensed with hydrazide to construct hydrazone **7**.

Crystallographic analysis confirmed the formation of *E*/*Z* isomers in telluroazole-based photoswitches (Fig. 2b, S28 and Table S1). In the *E*-**1** isomer, a Te···N chalcogen bond was observed with a distance of 2.99 Å, while the *Z*-**1** isomer exhibits intramolecular hydrogen bonding with an NH···N distance of 1.79 Å. Additionally, in the *E*-**7** isomer, the Te···N distance was found to be 3.25 Å, with a water molecule bound to hydrazone NH and CH *via* multiple hydrogen bonds. Notably, the *Z*-**4** isomer forms multiple NH hydrogen bonding with distances of 1.94 Å and 2.22 Å. These results highlight the impact of geometric isomerization on noncovalent interactions.

E/*Z* photoswitching studies

Firstly, single-crystal structural analysis validated the presence of an N–H···N hydrogen bond in the *Z*-**1** isomer, while this

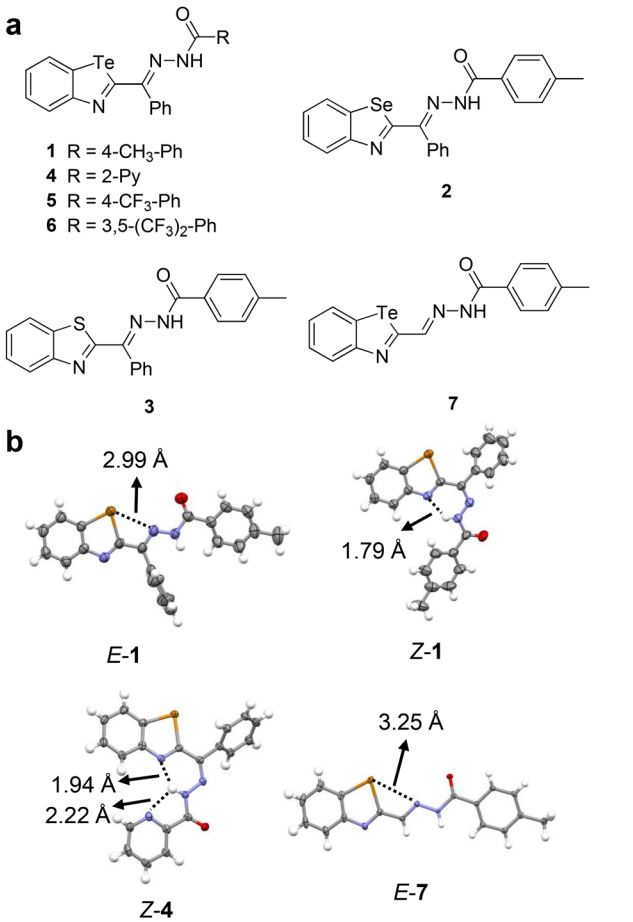

Fig. 2 (a) The hydrazone-based photoswitches studied in the current work. (b) Crystal structures of *E*-**1**, *Z*-**1**, *Z*-**4**, and *E*-**7**, with the distances of supramolecular contacts listed.

interaction is absent in the *E*-**1** isomer. As a result, the two isomers could be readily distinguished by the position of the NH peak in ^{1}H NMR spectroscopy. With this difference in mind, photoswitching behaviors were next investigated (Fig. S29–S58). Upon irradiation of *E*-**1** (a of Fig. 3A) in DMSO-d_6 at 313 nm for 30 minutes, $E \rightarrow Z$ isomerization was achieved, as evidenced by the emergence of a new NH signal at 15.31 ppm and a decrease in the original NH signal at 10.79 ppm (b of Fig. 3A). In the photostationary state (PSS), the content of 60% was found for the *Z*-isomer (Table 1). Further irradiation at 425 nm for 5 min induced efficient $Z \rightarrow E$ isomerization, affording 95% *E*-isomer in the PSS (c of Fig. 3A). The *E*/*Z* isomerization process was further corroborated by monitoring UV-vis spectra under 313 nm and 425 nm irradiation (Fig. 3B). Moreover, reversible interconversion between *E* and *Z* isomers was successfully realized through multiple cycles of alternating irradiation at 313 and 425 nm, demonstrating excellent reversibility and fatigue resistance for bidirectional photoswitching. In addition, the *Z*-**1** isomer exhibited high thermal stability, with a half-life ($t_{1/2}$) of 52 days at 25 °C (Fig. S40). The *E*/*Z* photoisomerization of other com-

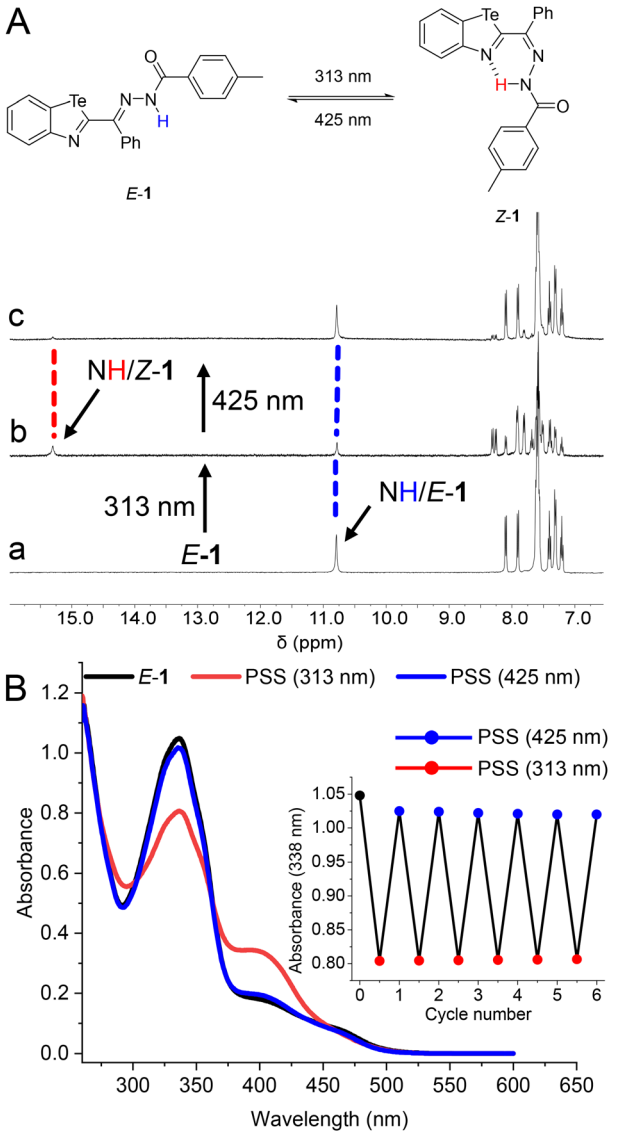

Fig. 3 (A) ^{1}H NMR spectra of *E*-**1** (5 mM) in DMSO-d_6 (a) upon irradiation at 313 nm (b) and then 425 nm (c). (B) Change of the absorbance spectra of *E*-**1** (50 μM) in DMSO upon irradiation at 313 nm and then 425 nm, with multiple cycles of switching in the inset.

Table 1 Summary of *E*/*Z* isomer ratios in the photostationary state (PSS) upon irradiation of hydrazone photoswitches

Compound	Isomer yield in the PSS[a] (at irr. λ in nm, time to reach the PSS in min)
1	60% *Z* (313, 30), 95% *E* (425, 5)
2	60% *Z* (313, 20), 95% *E* (425, 6)
3	67% *Z* (313, 15), 70% *E* (425, 9)
4	40% *Z* (313, 35)
5	50% *Z* (313, 25), 100% *E*(425, 4)
6	50% *Z* (313, 25), 100% *E*(425, 4)
7	60% *Z* (313, 40), 92% *E* (425, 5)

[a] To estimate PSS composition, ^{1}H NMR spectral data were recorded in DMSO-d_6 at a concentration of 5 mM.

pounds was also investigated under 313 nm and 425 nm irradiation in DMSO (Table 1). The results showed that most compounds afforded moderate $E \rightarrow Z$ isomerization efficiency upon 313 nm irradiation, with *Z*-isomer contents in the PSS ranging from 45% to 67%. Compound **3** gave the highest *Z*-isomer percentage (67%) under these conditions. With 425 nm illumination, most compounds exhibited highly efficient $Z \rightarrow E$ isomerization, yielding *E*-isomer contents between 92% and 100%. In particular, compounds **5** and **6** achieved nearly quantitative $Z \rightarrow E$ conversion (~100% *E*) under 425 nm irradiation. In contrast, compounds **3** and **4** showed lower $Z \rightarrow E$ conversion efficiency, affording 60% and 70% *E*-isomer, respectively. Overall, these results demonstrate that the studied acylhydrazone compounds exhibit bidirectional configurational photoswitching, with the substituents playing a significant role in modulating *E*/*Z* isomerization efficiency.

Anion binding studies

Having attained *E*/*Z* photoswitching, we further systematically evaluated the anion binding affinity of *E* and *Z* isomers through ^{1}H NMR titration experiments combined with binding isotherm analysis (Fig. 4a and S59–S75, Table S2). Tetrabutylammonium salts (TBACl, TBABr, and TBAI) were used as anionic guests. Initially, the anion binding properties of *E*-**1** (Fig. 4b) and *Z*-**1** (Fig. 4c) were examined in DMSO-d_6. The anion recognition was followed by tracking peak movement of aromatic protons (H_a) adjacent to tellurium, and the binding constants (K_a) were obtained by fitting into a 1 : 1 binding model according to the Job's plot (Fig. S59 and S60). Compared to *E*-**1** and chloride ($K_{a,E}$(Cl) = 1.00 M^{-1}) (Table 2),

Table 2 Binding constants (K_a, M^{-1}) of hydrazone compounds **1–7** with halide anions in DMSO-d_6 and *Z*/*E* binding affinity ratios (using Cl^- as the example)

Compound	K_a (M^{-1})			Selectivity[a]
	Cl^-	Br^-	I^-	Cl^-
E-**1**	1.00	0.62	nd[b]	4.79
Z-**1**	4.79	3.22	1.22	
E-**2**	nd	nd	nd	nd
Z-**2**[c]	1.09	0.30	nd	
E-**3**[c]	nd	nd	nd	nd
Z-**3**[c]	0.58	nd	nd	
E-**4**	0.98	0.57	nd	4.65
Z-**4**	4.56	2.82	1.05	
E-**5**	0.70	nd	nd	9.40
Z-**5**[c]	6.55	4.45	1.94	
E-**6**	0.76	nd	nd	11.12
Z-**6**	8.45	5.80	2.12	
E-**7**	5.36	nd	nd	0.48
Z-**7**	2.55	nd	nd	

[a] Selectivity = $K_{a,Z}/K_{a,E}$. [b] "nd" indicates that the binding constant is too small to be determined by fitting. [c] Titration was performed under conditions where both *Z* and *E* isomers coexist. The error of K_a was within 10%.

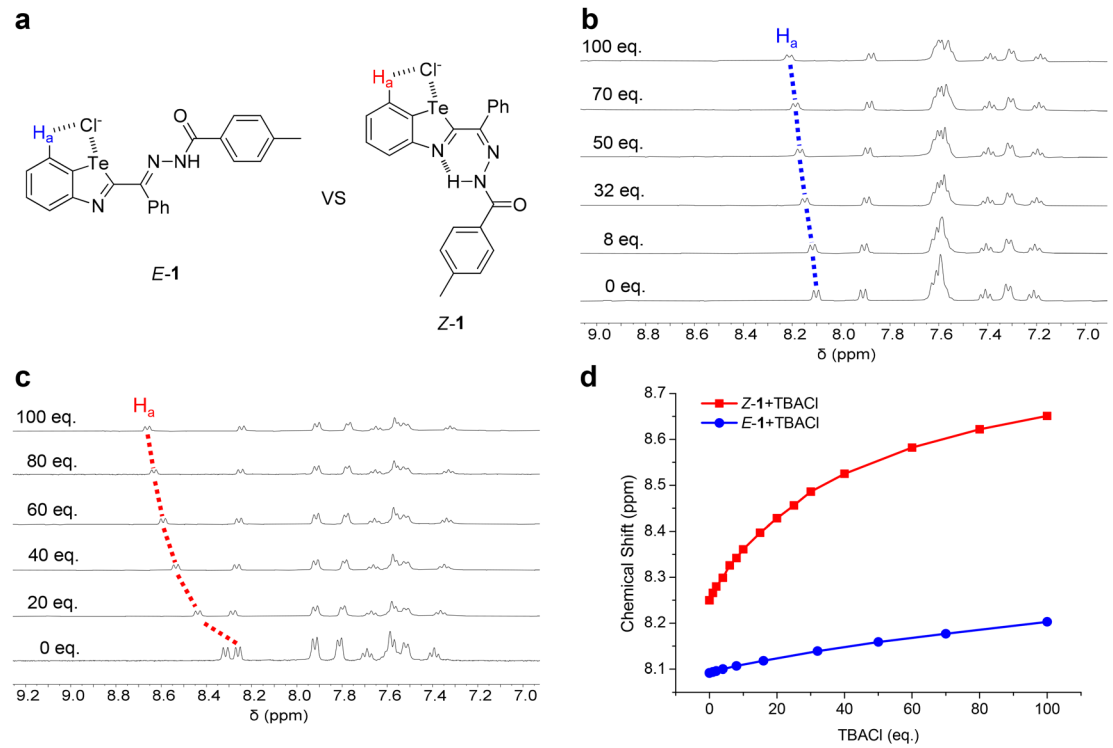

Fig. 4 (a) Schematic illustration of halide anion recognition modes for *E*-**1** and *Z*-**1**. ^{1}H NMR spectra of *E*-**1** (5 mM) (b) and *Z*-**1** (5 mM) (c) with different equivalents of TBACl in DMSO-d_6. (d) The comparison of changes in aromatic proton (H_a) chemical shifts of *E*-**1** and *Z*-**1** upon titrating TBACl.

Z-**1** exhibited significantly enhanced binding affinity toward chloride ($K_{a,Z}$(Cl) = 4.79 M^{-1}) (Fig. 4d). A similar trend was revealed for bromide, with a higher *K* value for *Z*-**1** ($K_{a,Z}$(Br) = 3.22 M^{-1}) over *E*-**1** ($K_{a,E}$(Br) = 0.62 M^{-1}). In addition, measurable affinity for *Z*-**1** and iodide was found ($K_{a,Z}$(I) = 1.22 M^{-1}), but not for *E*-**1**.

The enhancement in anion binding affinity for *Z*-**1** over *E*-**1** is rationalized with the electrophilic activation of the tellurazole unit in *Z*-**1** by NH···N HB, which increases its electron deficiency and thereby enhances its ability to recognize halide anions *via* ChB. Moreover, anion-induced ChB would also strengthen NH···N HB, leading to a synergistic effect between noncovalent interactions. Such activation is infeasible in *E*-**1** due to its extended geometry.

For compounds **2** and **3** the binding affinity decreases significantly as the chalcogen atom is sequentially replaced from Te to Se and then to S, reflecting gradual weakening of the ChB strength across the series (Table 2). In DMSO-d_6, *Z*-**2** exhibited a *K* value of 1.09 M^{-1} with Cl^- and a *K* value of 0.30 M^{-1} with bromide, and no detectable binding was observed for iodide. The binding affinity of **3** is further reduced, with *Z*-**3** showing a *K* value of only 0.58 M^{-1} with chloride and negligible binding toward bromide and iodide. This trend indicates a progressive decline in anion recognition capability as the chalcogen bond donor shifts from tellurium to selenium to sulfur.

Halide binding was observed for *Z*-**4** ($K_{a,Z}$(Cl) = 4.56 M^{-1}, $K_{a,Z}$(Br) = 2.82 M^{-1}, $K_{a,Z}$(I) = 1.05 M^{-1}), showing a comparable affinity to *Z*-**1** (Table 2). The incorporation of electron-withdrawing substituents (*E*-**5**/*Z*-**5** and *E*-**6**/*Z*-**6**) resulted in enhancement in binding affinity. *Z*-**5** afforded a *K* value of 6.55 M^{-1} for chloride, along with increased affinity for bromide ($K_{a,Z}$(Br) = 4.45 M^{-1}) and iodide ($K_{a,Z}$(I) = 1.94 M^{-1}). *Z*-**6** exhibited the strongest binding affinity in the series ($K_{a,Z}$(Cl) = 8.45 M^{-1}, $K_{a,Z}$(Br) = 5.80 M^{-1}, $K_{a,Z}$(Br) = 2.12 M^{-1}). Compared to their corresponding *E* isomers ($K_{a,E}$(Cl) = 0.70–0.76 M^{-1}), both *Z*-**5** and *Z*-**6** showed significant enhancement, with up to an 11-fold increase in binding affinity. Overall, in DMSO-d_6, *Z* isomers from the ketone-derived hydrazones consistently exhibited stronger chloride binding than their *E* counterparts. *Z*-**6** displayed the highest chloride binding constant (8.45 M^{-1}), with a $K_{a,Z}/K_{a,E}$ ratio of 11.1. Opposite to **1–6**, a higher *K* value with chloride was apparent for the aldehyde-derived hydrazones *E*-**7** (5.36 M^{-1}) over *Z*-**7** (2.55 M^{-1}). With HB from NH of the hydrazone contributing to anion recognition in *E*-**7** but not *Z*-**7**, the trend would be reversed. Nearly no NH movement was found for *E*-**1** upon adding an anion, whereas a notable one was apparent for *E*-**7** (Fig. S76).[58,59] Such a difference supports the effect of the phenyl group directing anion binding toward chalcogen. These results demonstrate that *E* → *Z* isomerization enhances halide recognition, essentially accomplishing light-responsive anion receptors.

As a means of enhancing binding affinity discrimination between *E*/*Z* isomers, anion recognition was evaluated in various solvents, including DMSO-d_6, CD_2Cl_2, and CD_3CN/DMSO-d_6 (4 : 1). In CD_2Cl_2, the *K* values of *Z*-**1** with Cl^- were found to be 3.90 M^{-1}, respectively (Fig. S68). The value is smaller than the data in DMSO-d_6. Although intramolecular HB could be favored in solvents of lower polarity, the polarization of the N–H bond and hence HB activation would be compromised. For **1** the chloride binding constant of *Z*-**1** reached 10.15 M^{-1} in CD_3CN/DMSO-d_6 (4 : 1), significantly higher than that of *E*-**1** (1.27 M^{-1}) and giving a $K_{a,Z}/K_{a,E}$ ratio of approximately 8.0 (Table 3). Similarly, *Z*-**4** exhibited a *K* value of 9.52 M^{-1} for Cl^- in CD_3CN/DMSO-d_6 (4 : 1), whereas *E*-**4** showed a lower binding constant of 1.24 M^{-1} (a $K_{a,Z}/K_{a,E}$ ratio of around 7.68). Interestingly, further introduction of electron-withdrawing substituents led to an increase in both the $K_{a,Z}$ value and $K_{a,Z}/K_{a,E}$ ratio. *Z*-**5** showed a Cl^- binding constant of 21.03 M^{-1} in CD_3CN/DMSO-d_6 (4 : 1), much higher than that of *E*-**5** (1.08 M^{-1}) and corresponding to a $K_{a,Z}/K_{a,E}$ ratio of 19.5. Again *Z*-**6** exhibited the highest Cl^- binding constant among the series, reaching 25.66 M^{-1}, while *E*-**6** with Cl^- remained at 1.28 M^{-1} (a $K_{a,Z}/K_{a,E}$ ratio of around 23.0). Similar trends were observed in the binding of Br^- and I^-. In CD_3CN/DMSO-d_6 (4 : 1), *Z*-**5** showed *K* values of 12.71 M^{-1} (Br^-) and 6.79 M^{-1} (I^-), while *Z*-**6** gave *K* values of 14.17 M^{-1} (Br^-) and 8.83 M^{-1} (I^-), surpassing the other *Z* isomers.

Density functional theory (DFT) calculations further shed light on the molecular conformation and anion binding mode (Fig. S77–S81). The optimized structures of compound **1** fall in line with the crystal data, and *E*-**1** is energetically favored over *Z*-**1** by 0.28 kcal mol^{-1} (Fig. 5a). Intriguingly, anion binding induces the reversal of energy, stabilizing *Z*-**1** by 0.71 kcal mol^{-1}. *E*-**1**(Cl^-) displays Te···Cl^- ChB (3.04 Å) and C–H···Cl^- HB (2.53 Å) with natural bonding orbital (NBO) analysis giving the estimation of interacting strength of ChB (16.13 kcal mol^{-1}) and HB (2.67 kcal mol^{-1}) energies (Fig. 5b). While maintaining C–H···Cl^- HB (2.53 Å, 2.57 kcal mol^{-1}), *Z*-**1**(Cl^-) exhibits a stronger ChB (2.96 Å, 21.05 kcal mol^{-1}). This is due to the synergistic effect between ChB and N–H···N HB (1.80 Å, 19.83 kcal), leading to the stabilization of the *Z* isomer complex. Upon chloride bonding, the N–H···N HB (19.83 kcal

Table 3 Binding constants (K_a, M^{-1}) of hydrazone compounds **1**, **4**, **5**, and **6** with halide anions in CD_3CN/DMSO-d_6 (4 : 1) and *Z*/*E* binding affinity ratios (using Cl^- as the example)

Compound	K_a (M^{-1})			Selectivity[a]
	Cl^-	Br^-	I^-	Cl^-
E-**1**	1.27	1.19	1.05	7.99
Z-**1**	10.15	6.07	4.35	
E-**4**	1.24	1.09	0.94	7.68
Z-**4**	9.52	5.69	4.20	
E-**5**[c]	1.08	nd[b]	nd	19.47
Z-**5**[c]	20.03	12.71	6.79	
E-**6**[c]	1.28	nd	nd	23.12
Z-**6**	25.66	14.17	8.83	

[a] Selectivity = $K_{a,Z}/K_{a,E}$. [b] "nd" indicates that the binding constant is too small to be determined by fitting. [c] Titration was performed under conditions where both *Z* and *E* isomers coexist. The error of K_a was within 10%.

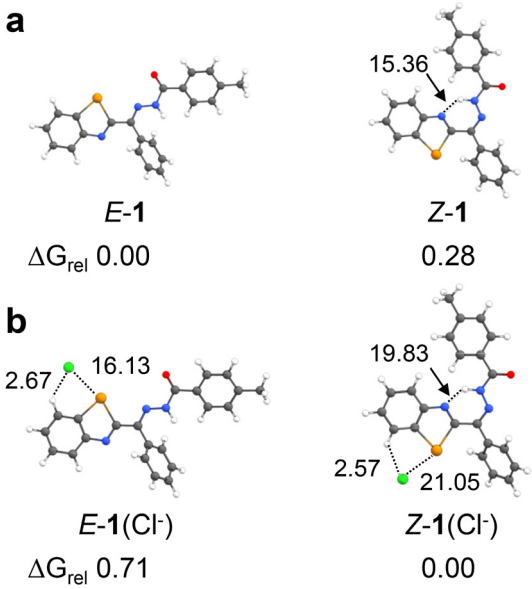

Fig. 5 The molecular conformation and anion binding mode for compound **1**. (a) Optimized structures of *E* and *Z* isomers for compound **1** (a) and complex **1** (Cl^-) (b), with the relative energies and NBO energies (kcal/mol) listed, respectively.

mol^{-1}) in *Z*-**1**(Cl^-) is strengthened over that in *Z*-**1** (15.36 kcal mol^{-1}), further supporting the cooperativity between HB and ChB. Two σ-holes locate on the chalcogen atom, with this arrangement of Cl^- energetically favored over the other site (>4 kcal mol^{-1}) for both *E* and *Z* isomers (Fig. S79). The non-covalent interaction plot further validated the attractive interaction of chloride anion lone pairs with different electron acceptors (Fig. S81). The N–H···N HB from pyridine in *Z*-**4** has a competitive effect on N–H···N (telluroazole) HB, slightly weakening the ChB (Fig. S78 and S80). Differently, the introduction of electron-withdrawing groups in *Z*-**5** strengthens the N–H···N HB and ChB, resulting from the enhanced polarization of the N–H bond (Fig. S78 and S80). These computational results are consistent with the trend of the anion recognition affinity.

Altogether, the systematic studies demonstrate that *E* → *Z* isomerization of the ketone-derived acylhydrazones enhances anion binding affinity across a range of chalcogen-containing receptors and solvents. The binding constant increases with the heavier chalcogen atoms (Te > Se > S), matching the intrinsic trend of chalcogen bond strength. The introduction of electron-withdrawing substituents further amplifies the binding enhancement by increasing bond polarization. Across different solvents studied, *Z* isomers show superior binding over *E* isomers, with the most significant enhancements observed in CD_3CN/DMSO-d_6 (4 : 1). In solvents of medium polarity, a delicate balance would be reached for NH activation, maintaining intramolecular HB against competition from solvents. The participation of NH HB in binding anions with *Z* isomers of **1**–**6** is unlikely due to the hindrance arising from the phenyl group. These findings underscore the collective role of chalcogen bonding, hydrogen bonding, electronic modulation, and steric effects toward achieving photoresponsive anion recognition.

The effects of anions on photoswitching

Finally, we explored the impact of anion binding and ChB on *E*/*Z* isomerization.[90–93] In CD_3CN/DMSO-d_6 (4 : 1), compound **1** underwent *E* → *Z* isomerization upon irradiation at 313 nm, reaching the PSS with 70% of the *Z* isomer (Fig. S82–S102). Conversely, irradiation at 425 nm induced *Z* → *E* isomerization (Fig. 6A), yielding 60% of the *E* isomer in the PSS. The *Z* → *E* photoisomerization efficiency at 425 nm was significantly enhanced in the presence of anions: upon addition of 10 equivalents of Cl^-, the *Z* → *E* conversion in the PSS reached 98% (Fig. 6B). The improvement in *Z* → *E* switching was also feasible with Br^- and I^-. This phenomenon is interpreted with anion-induced electronic effects. Spectroscopically, halide coordination leaves absorption maxima (λ_{max}) virtually unchanged but amplifies the *E*/*Z* dipole moment difference ($\Delta\mu$) 9.5-fold (1.4 → 13.3 Debye, Table S3), reflecting significant polarity redistribution upon switching. Considering the enhanced anion binding for the *Z* isomer, the increased polarization of the receptor alters the electronic environment of the photoswitchable acylhydrazone unit,[94–96] thereby improving its responsiveness to 425 nm light and facilitating the *Z* → *E* isomerization process. UV-vis spectral measurement after 313 nm and 425 nm irradiation further confirmed the reversible nature of *E*/*Z* photoisomerization in the presence of anions.

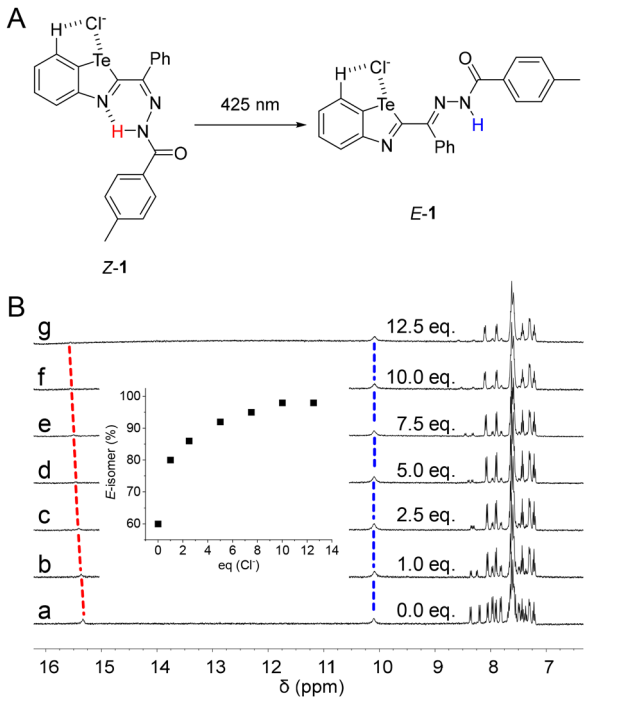

Fig. 6 (A) The effects of anion binding on the *E*/*Z* isomerization of compound **1**. (B) (a)–(f) ^{1}H NMR spectra of the PSS obtained from *Z* → *E* isomerization upon irradiation of *Z*-**1** (5 mM) with different equivalents of TBACl at 425 nm in CD_3CN/DMSO-d_6 (4 : 1), with the change in the percentage of *E*-**1** in the inset.

Repeated alternating irradiation with 313 nm and 425 nm light enabled the interconversion between *E* and *Z* isomers, demonstrating excellent fatigue resistance (Fig. S92 and S93). Moreover, the thermal stability of the *Z*-**1** isomer was improved with chloride present, extending the half-life ($t_{1/2}$) to 73 days at 25 °C (Fig. S99). As a result, anion recognition offered a facile route for tuning *E*/*Z* switching.

Conclusion

In summary, we reported photoresponsive molecular receptors integrating a telluroazole-based chalcogen bond donor with hydrazone photoswitches to achieve light-controlled anion recognition. The reversible *E*/*Z* isomerization not only modulates the formation and disruption of a key intramolecular hydrogen bond but also significantly influences the electrophilicity of the chalcogen bond donor, leading to enhanced anion binding in the *Z* isomer. The introduction of electron-withdrawing aromatic substituents and the change of solvents further amplify the polarization effect, enabling fine-tuning of binding affinity and selectivity. Binding studies revealed that the *Z* isomer exhibits up to a 20-fold increase in halide anion binding affinity compared to the *E* isomer, demonstrating a synergistic enhancement between hydrogen bonding and chalcogen bonding under photochemical control. Moreover, anion binding promotes $Z \rightarrow E$ photoisomerization, uncovering a feedback mechanism between anion recognition and photoisomerization. This work proposed an innovative strategy combining reversible photochemical switching with cooperative noncovalent interactions to achieve controllable anion recognition. The results should pave the way for future design and applications in molecular recognition, chemical sensing, ion transport, and smart materials.

Author contributions

Q. R. carried out the synthetic work, photoswitching studies, and titration experiments. H. Y. carried out the theoretical calculation and analysed the data. L. Y. designed and supervised the project. All authors discussed the results, wrote the manuscript, and have given approval to the final version of the manuscript.

Conflicts of interest

There are no conflicts to declare.

Data availability

All relevant data are within the manuscript and its supplementary information (SI). Supplementary information: experimental details, X-ray, NMR, UV-vis spectra, and computational data. See DOI: **https://doi.org/10.1039/d5qo01341k**.

CCDC 2457219–2457222 contain the supplementary crystallographic data for this paper.[97a–d]

Acknowledgements

We thank NSFC (22471274, 22101283, 22101284, and 92156010), the Strategic Priority Research Program (XDB1170000) of the CAS, NSF of Fujian Province (2020J06035 and 2022J05085), and the Fujian Science & Technology Innovation Laboratory for Optoelectronic Information of China (2021ZR112) for funding.

References

1 A. Blanco-Gómez, P. Cortón, L. Barravecchia, I. Neira, E. Pazos, C. Peinador and M. D. García, Controlled binding of organic guests by stimuli-responsive macrocycles, *Chem. Soc. Rev.*, 2020, **49**, 3834–3862.
2 C. Kremer and A. Lützen, Artificial Allosteric Receptors, *Chem. – Eur. J.*, 2013, **19**, 6162–6196.
3 J.-X. Liu, K. Chen and C. Redshaw, Stimuli-responsive mechanically interlocked molecules constructed from cucurbit[n]uril homologues and derivatives, *Chem. Soc. Rev.*, 2023, **52**, 1428–1455.
4 M. Han, R. Michel, B. He, Y.-S. Chen, D. Stalke, M. John and G. H. Clever, Light-Triggered Guest Uptake and Release by a Photochromic Coordination Cage, *Angew. Chem., Int. Ed.*, 2013, **52**, 1319–1323.
5 T. Dünnebacke, N. Niemeyer, S. Baumert, S. Hochstädt, L. Borsdorf, M. R. Hansen, J. Neugebauer and G. Fernández, Molecular and supramolecular adaptation by coupled stimuli, *Nat. Commun.*, 2024, **5695**, 15.
6 Y.-H. Song, Q. Bian, F. Wang, J. Liu, Y.-H. Yang, Y.-M. Zhang and Y. Liu, Water-soluble stimuli-responsive supramolecular nanoagrochemicals based on macrocycle compounds, *Coordin. Chem. Rev.*, 2025, **524**, 216299.
7 S. Panja and D. J. Adams, Stimuli responsive dynamic transformations in supramolecular gels, *Chem. Soc. Rev.*, 2021, **50**, 5165–5200.
8 C. Pezzato, C. Cheng, J. F. Stoddart and R. D. Astumian, Mastering the non-equilibrium assembly and operation of molecular machines, *Chem. Soc. Rev.*, 2017, **46**, 5491–5507.
9 S.-L. Qiao, M. Mamuti, H.-W. An and H. Wang, Thermoresponsive Polymer Assemblies: From Molecular Design to Theranostics Application, *Prog. Polym. Sci.*, 2022, **131**, 101578.
10 M. Martínez-Orts and S. Pujals, Responsive Supramolecular Polymers for Diagnosis and Treatment, *Int. J. Mol. Sci.*, 2024, **25**, 4077.
11 F. Xu, L. Pfeifer, S. Crespi, F. K.-C. Leung, M. C. A. Stuart, S. J. Wezenberg and B. L. Feringa, From Photoinduced Supramolecular Polymerization to Responsive Organogels, *J. Am. Chem. Soc.*, 2021, **143**, 5990–5997.

12 S. Song, H. Zhang and Y. Liu, Light-Controlled Macrocyclic Supramolecular Assemblies and Luminescent Behaviors, *Acc. Mater. Res.*, 2024, **5**, 1109–1120.
13 F. Xu and B. L. Feringa, Photoresponsive Supramolecular Polymers: From Light-Controlled Small Molecules to Smart Materials, *Adv. Mater.*, 2023, **35**, 2204413.
14 J.-L. Zhao, M.-H. Li, Y.-M. Cheng, X.-W. Zhao, Y. Xu, Z.-Y. Cao, M.-H. You and M.-J. Lin, Photochromic crystalline hybrid materials with switchable properties: Recent advances and potential applications, *Coordin. Chem. Rev.*, 2023, **475**, 214918.
15 B. D. Fairbanks, L. J. Macdougall, S. Mavila, J. Sinha, B. E. Kirkpatrick, K. S. Anseth and C. N. Bowman, Photoclick Chemistry: A Bright Idea, *Chem. Rev.*, 2021, **121**, 6915–6990.
16 H. Frisch, D. E. Marschner, A. S. Goldmann and C. Barner-Kowollik, Wavelength-Gated Dynamic Covalent Chemistry, *Angew. Chem., Int. Ed.*, 2018, **57**, 2036–2045.
17 M. Kathan and S. Hecht, Photoswitchable molecules as key ingredients to drive systems away from the global thermodynamic minimum, *Chem. Soc. Rev.*, 2017, **46**, 5536–5550.
18 D.-H. Qu, Q.-C. Wang, Q.-W. Zhang, X. Ma and H. Tian, Photoresponsive Host–Guest Functional Systems, *Chem. Rev.*, 2015, **115**, 7543–7588.
19 J. Quan, Y. Guo, J. Ma, D. Long, J. Wang, L. Zhang, Y. Sun, M. K. Dhinakaran and H. Li, Light-responsive nanochannels based on the supramolecular host–guest system, *Front. Chem.*, 2022, **10**, 986908.
20 L. Wang, H. Zou, H. Ye, Y. Hai, H. Lu, J. Deng and L. You, Photoswitchable Molecular Recognition Enabled by Dithienylethene-Mediated Structural Changes of Dynamic Covalent Hydrazone Bonds, *CCS Chem.*, 2024, **6**, 497–506.
21 L. Wei, S.-T. Han, T.-T. Jin, T.-G. Zhan, L.-J. Liu, J. Cui and K.-D. Zhang, Towards photoswitchable quadruple hydrogen bonds via a reversible "photolocking" strategy for photocontrolled self-assembly, *Chem. Sci.*, 2021, **12**, 1762–1771.
22 Z. Yang, Z. Liu and L. Yuan, Recent Advances of Photoresponsive Supramolecular Switches, *Asian J. Org. Chem.*, 2021, **10**, 74–90.
23 B. Yao, H. Sun, L. Yang, S. Wang and X. Liu, Recent Progress in Light-Driven Molecular Shuttles, *Front. Chem.*, 2022, **9**, 832735.
24 D. Dattler, G. Fuks, J. Heiser, E. Moulin, A. Perrot, X. Yao and N. Giuseppone, Design of Collective Motions from Synthetic Molecular Switches, Rotors, and Motors, *Chem. Rev.*, 2020, **120**, 310–433.
25 Y. Deng, G. Long, Y. Zhang, W. Zhao, G. Zhou, B. L. Feringa and J. Chen, Photo-responsive functional materials based on light-driven molecular motors, *Light: Sci. Appl.*, 2024, **13**, 63.
26 S. C. Patrick, P. D. Beer and J. J. Davis, Solvent effects in anion recognition, *Nat. Rev. Chem.*, 2024, **8**, 256–276.
27 N. Busschaert, C. Caltagirone, W. Van Rossom and P. A. Gale, Applications of Supramolecular Anion Recognition, *Chem. Rev.*, 2015, **115**, 8038–8155.
28 D.-X. Wang and M.-X. Wang, Exploring Anion–π Interactions and Their Applications in Supramolecular Chemistry, *Acc. Chem. Res.*, 2020, **53**, 1364–1380.
29 X. Wu, A. M. Gilchrist and P. A. Gale, Prospects and Challenges in Anion Recognition and Transport, *Chem*, 2020, **6**, 1296–1309.
30 J. Pancholi and P. D. Beer, Halogen bonding motifs for anion recognition, *Coordin. Chem. Rev.*, 2020, **416**, 213281.
31 J. Zhao, D. Yang, X.-J. Yang and B. Wu, Anion coordination chemistry: From recognition to supramolecular assembly, *Coordin. Chem. Rev.*, 2019, **378**, 415–444.
32 P. Molina, F. Zapata and A. Caballero, Anion Recognition Strategies Based on Combined Noncovalent Interactions, *Chem. Rev.*, 2017, **117**, 9907–9972.
33 M. S. Taylor, Anion recognition based on halogen, chalcogen, pnictogen and tetrel bonding, *Coordin. Chem. Rev.*, 2020, **413**, 213270.
34 P. A. Gale, Anion and ion-pair receptor chemistry: highlights from 2000 and 2001, *Coordin. Chem. Rev.*, 2003, **240**, 191–221.
35 N. Biot and D. Bonifazi, Chalcogen-bond driven molecular recognition at work, *Coordin. Chem. Rev.*, 2020, **413**, 213243.
36 G. R. Gleiter, G. Haberhauer, D. B. Werz, F. Rominger and C. Bleiholder, From Noncovalent Chalcogen-Chalcogen Interactions to Supramolecular Aggregates: Experiments and Calculations, *Chem. Rev.*, 2018, **118**, 2010–2041.
37 K. T. Mahmudov, A. V. Gurbanov, V. A. Aliyeva, M. F. C. G. da Silva, G. Resnati and A. J. L. Pombeiro, Chalcogen bonding in coordination chemistry, *Coordin. Chem. Rev.*, 2022, **464**, 214556.
38 G. Sekar, V. V. Nair and J. Zhu, Chalcogen bonding catalysis, *Chem. Soc. Rev.*, 2024, **53**, 586–605.
39 P. Pale and V. Mamane, Chalcogen Bonding Catalysis: Tellurium, the Last Frontier?, *Chem. – Eur. J.*, 2023, **29**, e202302755.
40 D. J. Pascoe, K. B. Ling and S. L. Cockroft, The Origin of Chalcogen-Bonding Interactions, *J. Am. Chem. Soc.*, 2017, **139**, 15160–15167.
41 A. Docker, Y. C. Tse, H. M. Tay, Z. Zhang and P. D. Beer, Ammonium halide selective ion pair recognition and extraction with a chalcogen bonding heteroditopic receptor, *Dalton Trans.*, 2024, **53**, 11141–11146.
42 J. Y. C. Lim and P. D. Beer, Sigma-Hole Interactions in Anion Recognition, *Chem*, 2018, **4**, 731–783.
43 J. Y. C. Lim, I. Marques, A. L. Thompson, K. E. Christensen, V. Félix and P. D. Beer, Chalcogen Bonding Macrocycles and [2]Rotaxanes for Anion Recognition, *J. Am. Chem. Soc.*, 2017, **139**, 3122–3133.
44 K. T. Mahmudov, M. N. Kopylovich, M. F. C. G. da Silva and A. J. L. Pombeiro, Chalcogen bonding in synthesis, catalysis and design of materials, *Dalton Trans.*, 2017, **46**, 10121–10138.
45 L. Vogel, P. Wonner and S. M. Huber, Chalcogen Bonding: An Overview, *Angew. Chem., Int. Ed.*, 2019, **58**, 1880–1891.

46 X. Liu, G. Liu, T. Fu, K. Ding, J. Guo, Z. Wang, W. Xia and H. Shangguan, Structural Design and Energy and Environmental Applications of Hydrogen-Bonded Organic Frameworks: A Systematic Review, *Adv. Sci.*, 2024, **11**, 2400101.
47 U. Manna and G. Das, An overview of anion coordination by hydroxyl, amine and amide based rigid and symmetric neutral dipodal receptors, *Coordin. Chem. Rev.*, 2021, **427**, 213547.
48 T. Vijayakanth, S. Dasgupta, P. Ganatra, S. Rencus-Lazar, A. V. Desai, S. Nandi, R. Jain, S. Bera, A. I. Nguyen, E. Gazit and R. Misra, Peptide hydrogen-bonded organic frameworks, *Chem. Soc. Rev.*, 2024, **53**, 3640–3655.
49 L. J. Karas, C.-H. Wu, R. Das and J. I.-C. Wu, Hydrogen bond design principles, *Wiley Interdiscip. Rev.: Comput. Mol. Sci.*, 2020, **10**, e1477.
50 G. Cavallo, P. Metrangolo, R. Milani, T. Pilati, A. Priimagi, G. Resnati and G. Terraneo, The Halogen Bond, *Chem. Rev.*, 2016, **116**, 2478–2601.
51 S. Lindblad, K. Mehmeti, A. X. Veiga, B. Nekoueishahraki, J. Gräfenstein and M. Erdélyi, Halogen Bond Asymmetry in Solution, *J. Am. Chem. Soc.*, 2018, **140**, 13503–13513.
52 L. Turunen, J. H. Hansen and M. Erdélyi, Halogen Bonding: An Odd Chemistry?, *Chem. Rec.*, 2021, **21**, 1252–1257.
53 S. De and S. Nag, Halogen bonding: a new territory for anion sensing, *Rev. Inorg. Chem.*, 2025, DOI: **10.1515/revic-2025-0015**.
54 J. D. Einkauf, V. S. Bryantsev, B. A. Moyer and R. Custelcean, A Photoresponsive Receptor with a 10^5 Magnitude of Reversible Anion-Binding Switching, *Chem. – Eur. J.*, 2022, **28**, e202200719.
55 M. Ahmad, M. Flerin, H. M. Tay, A. L. Thompson, F. Duarte and M. J. Langton, Stimuli-responsive anion transport utilising caged hydrazone-based anionophores, *Nanoscale*, 2024, **16**, 21545–21553.
56 G. Vantomme and J.-M. Lehn, Photo- and Thermoresponsive Supramolecular Assemblies: Reversible Photorelease of K^+ Ions and Constitutional Dynamics, *Angew. Chem., Int. Ed.*, 2013, **52**, 3940–3943.
57 M. Ahmad, D. Mondal, N. J. Roy, T. Vijayakanth and P. Talukdar, Reversible Stimuli-Responsive Transmembrane Ion Transport Using Phenylhydrazone-Based Photoswitches, *ChemPhotoChem*, 2022, **6**, e202200002.
58 Z. Kokan and M. J. Chmielewski, A Photoswitchable Heteroditopic Ion-Pair Receptor, *J. Am. Chem. Soc.*, 2018, **140**, 16010–16014.
59 B. Shao, H. Fu and I. Aprahamian, A molecular anion pump, *Science*, 2024, **385**, 544–549.
60 P. Msellem, M. Dekthiarenko, N. Hadj Seyd and G. Vives, Switchable molecular tweezers: design and applications, *Beilstein J. Org. Chem.*, 2024, **20**, 504–539.
61 S. J. Wezenberg, M. Vlatković, J. C. M. Kistemaker and B. L. Feringa, Multi-State Regulation of the Dihydrogen Phosphate Binding Affinity to a Light- and Heat-Responsive Bis-Urea Receptor, *J. Am. Chem. Soc.*, 2014, **136**, 16784–16787.
62 D. Villarón, J. E. Bos, F. Kohl, S. Mommer, J. de Jong and S. J. Wezenberg, Photoswitchable Bis(amidopyrroles): Modulating Anion Transport Activity Independent of Binding Affinity, *J. Org. Chem.*, 2023, **88**, 11328–11334.
63 J. de Jong, B. L. Feringa and S. J. Wezenberg, Light-Modulated Self-Blockage of a Urea Binding Site in a Stiff-Stilbene Based Anion Receptor, *ChemPhysChem*, 2019, **20**, 3306–3310.
64 A. Kerckhoffs, I. Moss and M. J. Langton, Photo-switchable anion binding and catalysis with a visible light responsive halogen bonding receptor, *Chem. Commun.*, 2023, **59**, 51–54.
65 K. Dąbrowa, P. Niedbała and J. Jurczak, Engineering Light-Mediated Bistable Azobenzene Switches Bearing Urea d-Aminoglucose Units for Chiral Discrimination of Carboxylates, *J. Org. Chem.*, 2016, **81**, 3576–3584.
66 A. Kerckhoffs and M. J. Langton, Reversible photo-control over transmembrane anion transport using visible-light responsive supramolecular carriers, *Chem. Sci.*, 2020, **11**, 6325–6331.
67 S. Lee and A. H. Flood, Photoresponsive receptors for binding and releasing anions, *J. Phys. Org. Chem.*, 2013, **26**, 79–86.
68 J. Leng, G. Liu, T. Cui, S. Mao, P. Dong, W. Liu, X.-Q. Hao and M.-P. Song, Photoresponsive molecular tweezer: Control-release of anions and fluorescence switch, *Dyes Pigm.*, 2021, **184**, 108838.
69 A. Lutolli, M. Che, F. C. Parks, K. Raghavachari and A. H. Flood, Cooperativity in Photofoldamer Chloride Double Helices Turned On with Sequences and Solvents, Around with Guests, and Off with Light, *J. Org. Chem.*, 2023, **88**, 6791–6804.
70 D. Villarón and S. J. Wezenberg, Stiff-Stilbene Photoswitches: From Fundamental Studies to Emergent Applications, *Angew. Chem., Int. Ed.*, 2020, **59**, 13192–13202.
71 H.-Y. Duan, S.-T. Han, T.-G. Zhan, L.-J. Liu and K.-D. Zhang, Visible-Light-Switchable Tellurium-Based Chalcogen Bonding: Photocontrolled Anion Binding and Anion Abstraction Catalysis, *Angew. Chem., Int. Ed.*, 2023, **62**, e202212707.
72 H. Shan, W. Zhao, J. Wang, Y. Yao, H. Ma, K. Liu, X.-J. Yang and B. Wu, Manipulating the Isomerization of a Tris-azobenzene Cage by Anion Binding, *J. Am. Chem. Soc.*, 2025, **147**, 14960–14965.
73 J. Boekhoven, J. M. Poolman, C. Maity, F. Li, L. van der Mee, C. B. Minkenberg, E. Mendes, J. H. van Esch and R. Eelkema, Catalytic control over supramolecular gel formation, *Nat. Chem.*, 2013, **5**, 433–437.
74 S.-Y. Ding, M. Dong, Y.-W. Wang, Y.-T. Chen, H.-Z. Wang, C.-Y. Su and W. Wang, Thioether-Based Fluorescent Covalent Organic Framework for Selective Detection and Facile Removal of Mercury(II), *J. Am. Chem. Soc.*, 2016, **138**, 3031–3037.

75 J. F. Folmer-Andersen and J.-M. Lehn, Constitutional Adaptation of Dynamic Polymers: Hydrophobically Driven Sequence Selection in Dynamic Covalent Polyacylhydrazones, *Angew. Chem., Int. Ed.*, 2009, **48**, 7664–7667.
76 T. Jiao, G. Wu, Y. Zhang, L. Shen, Y. Lei, C.-Y. Wang, A. C. Fahrenbach and H. Li, Self-Assembly in Water with N-Substituted Imines, *Angew. Chem., Int. Ed.*, 2020, **59**, 18350–18367.
77 D. K. Kölmel and E. T. Kool, Oximes and Hydrazones in Bioconjugation: Mechanism and Catalysis, *Chem. Rev.*, 2017, **117**, 10358–10376.
78 Y. Li, J. Sui, L.-S. Cui and H.-L. Jiang, Hydrogen Bonding Regulated Flexibility and Disorder in Hydrazone-Linked Covalent Organic Frameworks, *J. Am. Chem. Soc.*, 2023, **145**, 1359–1366.
79 D.-W. Zhang, X. Zhao and Z.-T. Li, Aromatic Amide and Hydrazide Foldamer-Based Responsive Host-Guest Systems, *Acc. Chem. Res.*, 2014, **47**, 1961–1970.
80 I. Aprahamian, Hydrazone switches and things in between, *Chem. Commun.*, 2017, **53**, 6674–6684.
81 I. Cvrtila, H. Fanlo-Virgós, G. Schaeffer, G. Monreal Santiago and S. Otto, Redox Control over Acyl Hydrazone Photoswitches, *J. Am. Chem. Soc.*, 2017, **139**, 12459–12465.
82 D. J. van Dijken, P. Kovaříček, S. P. Ihrig and S. Hecht, Acylhydrazones as Widely Tunable Photoswitches, *J. Am. Chem. Soc.*, 2015, **137**, 14982–14991.
83 S. Erbas-Cakmak, S. D. P. Fielden, U. Karaca, D. A. Leigh, C. T. McTernan, D. J. Tetlow and M. R. Wilson, Rotary and linear molecular motors driven by pulses of a chemical fuel, *Science*, 2017, **358**, 340–343.
84 B. Shao and I. Aprahamian, Hydrazones as New Molecular Tools, *Chem*, 2020, **6**, 2162–2173.
85 L.-I. Socea, S.-F. Barbuceanu, E. M. Pahontu, A.-C. Dumitru, G. M. Nitulescu, R. C. Sfetea and T.-V. Apostol, Acylhydrazones and Their Biological Activity: A Review, *Molecules*, 2022, **27**, 8719.
86 X. Su and I. Aprahamian, Hydrazone-based switches, metallo-assemblies and sensors, *Chem. Soc. Rev.*, 2014, **43**, 1963–1981.
87 P. He, H. Ye, S. Jia, Q. Rao, Y. Zhou and L. You, Tellurazole/Tellurazolium Based Olefin Configurational Photoswitches Controlled by Noncovalent Interactions, *CCS Chem.*, 2025, **7**, 1698–1710.
88 E. Navarro-García, B. Galmés, M. D. Velasco, A. Frontera and A. Caballero, Anion Recognition by Neutral Chalcogen Bonding Receptors: Experimental and Theoretical Investigations, *Chem. – Eur. J.*, 2020, **26**, 4706–4713.
89 T. Chivers and R. S. Laitinen, Tellurium: a maverick among the chalcogens, *Chem. Soc. Rev.*, 2015, **44**, 1725–1739.
90 S. Jia, H. Ye, P. He, X. Lin and L. You, Selection of isomerization pathways of multistep photoswitches by chalcogen bonding, *Nat. Commun.*, 2023, **14**, 7139.
91 S. Mehrparvar, Z. N. Scheller, C. Wölper and G. Haberhauer, Design of Azobenzene beyond Simple On–Off Behavior, *J. Am. Chem. Soc.*, 2021, **143**, 19856–19864.
92 V. Josef, F. Hampel and H. Dube, Heterocyclic Hemithioindigos: Highly Advantageous Properties as Molecular Photoswitches, *Angew. Chem., Int. Ed.*, 2022, **61**, e202210855.
93 A. Kerckhoffs, K. E. Christensen and M. J. Langton, Fast relaxing red and near-IR switchable azobenzenes with chalcogen and halogen substituents: periodic trends, tuneable thermal half-lives and chalcogen bonding, *Chem. Sci.*, 2022, **13**, 11551–11559.
94 J. Filo, P. Tisovský, K. Csicsai, J. Donovalová, M. Gáplovský, A. Gáplovský and M. Cigáň, Tautomeric photoswitches: anion-assisted azo/azine-to-hydrazone photochromism, *RSC Adv.*, 2019, **9**, 15910–15916.
95 A. Rananaware, M. Samanta, R. S. Bhosale, M. A. Kobaisi, B. Roy, V. Bheemireddy, S. V. Bhosale, S. Bandyopadhyay and S. V. Bhosale, Photomodulation of fluoride ion binding through anion-π interactions using a photoswitchable azobenzene system, *Sci. Rep.*, 2016, **6**, 22928.
96 Y.-Z. Ma, J. D. Einkauf, X. Ma, D.-K. Dang, P. M. Zimmerman, R. Custelcean, B. Doughty and V. S. Bryantsev, Photoswitching dynamics of a guanidine anion receptor, *Phys. Chem. Chem. Phys.*, 2025, **27**, 13434–13446.
97 (*a*) CCDC 2457219: Experimental Crystal Structure Determination, 2025, DOI: **10.5517/ccdc.csd.cc2ngy47**; (*b*) CCDC 2457220: Experimental Crystal Structure Determination, 2025, DOI: **10.5517/ccdc.csd.cc2ngy58**; (*c*) CCDC 2457221: Experimental Crystal Structure Determination, 2025, DOI: **10.5517/ccdc.csd.cc2ngy69**; (*d*) CCDC 2457222: Experimental Crystal Structure Determination, 2025, DOI: **10.5517/ccdc.csd.cc2ngy7b**.